AD-A154 411 A METHOD FOR PREDICTING ADDITIVE DRAG REDUCTION FROM SMALL-DIAMETER PIPE..(U) DAVID W TAYLOR NAVAL SHIP RESEARCH AND DEVELOPMENT CENTER BET.. P S GRANVILLE 1/1

UNCLASSIFIED MAR 85 DTNSRDC/SPD-1142-01 F/G 20/4 NL

END

FILMED

DTIC

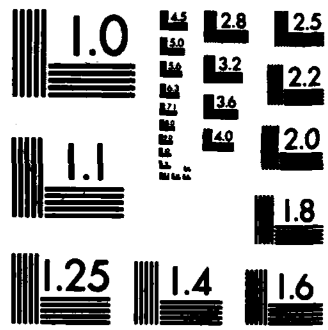

MICROCOPY RESOLUTION TEST CHART
NATIONAL BUREAU OF STANDARDS-1963-A

DTNSRDC/SPD-1142-01

A METHOD FOR PREDICTING ADDITIVE DRAG REDUCTION FROM SMALL-DIAMETER PIPE FLOWS

(2)

DAVID W. TAYLOR NAVAL SHIP RESEARCH AND DEVELOPMENT CENTER

Bethesda, Maryland 20084

A METHOD FOR PREDICTING
ADDITIVE DRAG REDUCTION
FROM SMALL-DIAMETER PIPE FLOWS

by

Paul S. Granville

APPROVED FOR PUBLIC RELEASE: DISTRIBUTION UNLIMITED

SHIP PERFORMANCE DEPARTMENT

DEPARTMENTAL REPORT

March 1985

DTNSRDC/SPD-1142-01

MAJOR DTNSRDC ORGANIZATIONAL COMPONENTS

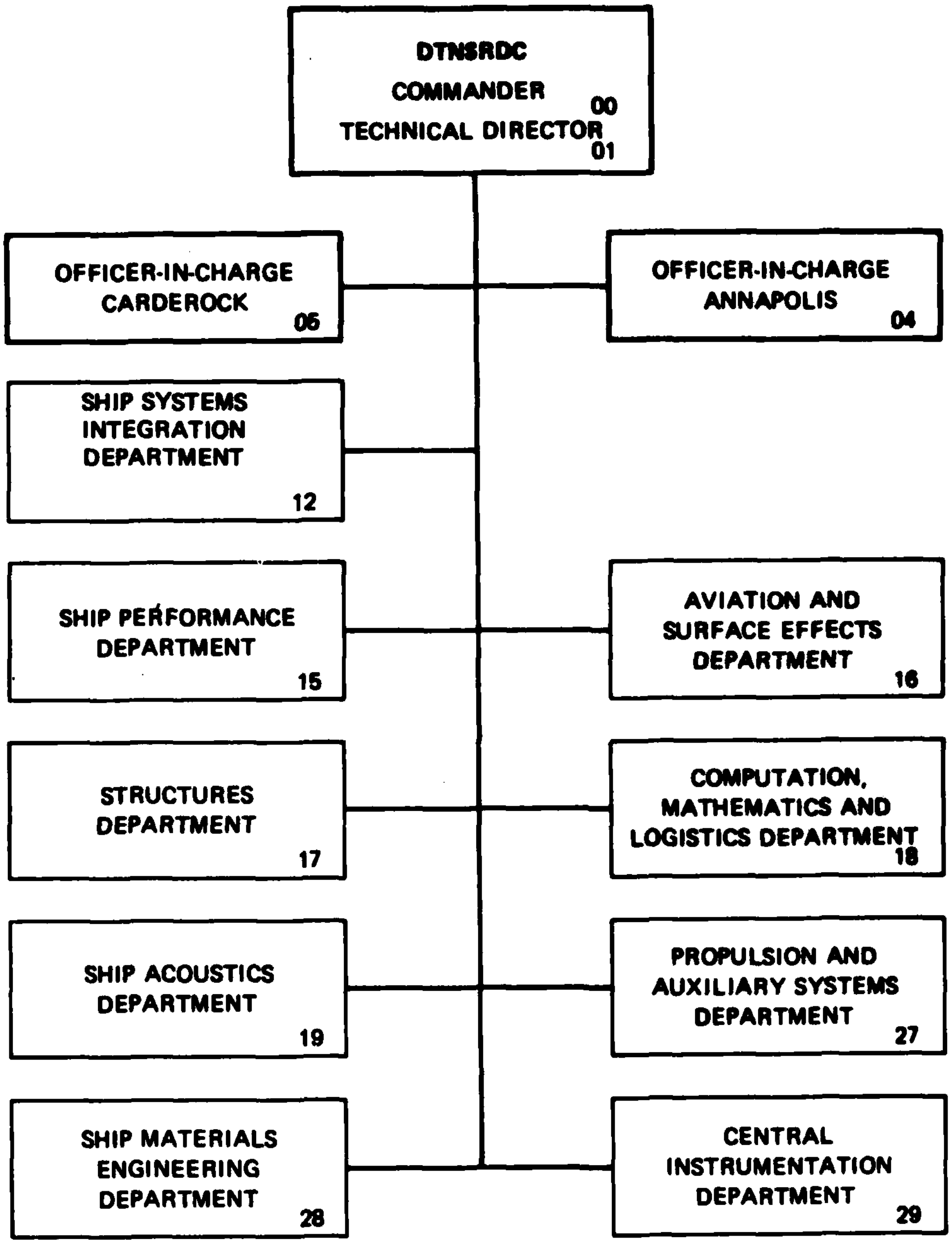

GPO 866 987

NDW-DTNSRDC 5602/21 (2-80)

UNCLASSIFIED
SECURITY CLASSIFICATION OF THIS PAGE

REPORT DOCUMENTATION PAGE

1a. REPORT SECURITY CLASSIFICATION UNCLASSIFIED	1b. RESTRICTIVE MARKINGS
2a. SECURITY CLASSIFICATION AUTHORITY	3. DISTRIBUTION/AVAILABILITY OF REPORT Approved for public release; distribution unlimited
2b. DECLASSIFICATION/DOWNGRADING SCHEDULE	
4. PERFORMING ORGANIZATION REPORT NUMBER(S) DTNSRDC/SPD-1142-01	5. MONITORING ORGANIZATION REPORT NUMBER(S)
6a. NAME OF PERFORMING ORGANIZATION David W. Taylor Naval Ship R&D Center 6b. OFFICE SYMBOL (If applicable) 1542	7a. NAME OF MONITORING ORGANIZATION David W. Taylor Naval Ship R&D Center Code 01
6c. ADDRESS (City, State, and ZIP Code) Bethesda, MD 20084-5000	7b. ADDRESS (City, State, and ZIP Code)
8a. NAME OF FUNDING/SPONSORING ORGANIZATION David W. Taylor Naval Ship R&D Center 8b. OFFICE SYMBOL (If applicable)	9. PROCUREMENT INSTRUMENT IDENTIFICATION NUMBER
8c. ADDRESS (City, State, and ZIP Code)	10. SOURCE OF FUNDING NUMBERS PROGRAM ELEMENT NO. 61152N PROJECT NO TASK NO. ZR0230101 WORK UNIT ACCESSION NO. 1542-140

11. TITLE (Include Security Classification)
(U) A Method for Predicting Additive Drag Reduction from Small-Diameter Pipe Flows

12. PERSONAL AUTHOR(S) Paul S. Granville

13a. TYPE OF REPORT	13b. TIME COVERED	14. DATE OF REPORT (Year, Month, Day)	15. PAGE COUNT
Final	FROM ______ TO ______	March 1985	

16. SUPPLEMENTARY NOTATION

17. COSATI CODES			18. SUBJECT TERMS (Continue on reverse if necessary and identify by block number)
FIELD	GROUP	SUB-GROUP	drag-reducing additives, pipe drag

19. ABSTRACT (Continue on reverse if necessary and identify by block number)

The method of two loci for scaling-up the drag reduction by additives from measurements in not-too-small diameter pipes is extended to small diameter pipes. This is accomplished by including the effects of the viscous sublayer and buffer layer in formulating a prediction chart. A mixing-length model proved more accurate than three other models of the viscous sublayer and buffer layer in a comparison of predictions with measured data. The prediction chart may also be used to obtain a similarity-law drag-reduction characterization.

20. DISTRIBUTION/AVAILABILITY OF ABSTRACT XX UNCLASSIFIED/UNLIMITED ☐ SAME AS RPT ☐ DTIC USERS	21. ABSTRACT SECURITY CLASSIFICATION UNCLASSIFIED
22a. NAME OF RESPONSIBLE INDIVIDUAL Paul S. Granville	22b. TELEPHONE (Include Area Code) 202/227-1410 22c. OFFICE SYMBOL 1542

DD FORM 1473, 84 MAR — 83 APR edition may be used until exhausted. All other editions are obsolete.

SECURITY CLASSIFICATION OF THIS PAGE
UNCLASSIFIED

TABLE OF CONTENTS

NOTATION

A	Slope of logarithmic similarity law
$\tilde{A}$	Slope of elastic-layer logarithmic law
$\hat{A}$	Type of additive
B_1	Intercept of logarithmic similarity law
$B_{1,0}$	B_1 for ordinary fluids
B_2	Velocity-defect factor
$\tilde{B}$	Intercept of elastic-layer logarithmic law
C	Concentration of additive
c_1, c_2	Constants
D	Diameter of pipe
f	Fanning friction factor
J	Factor in thick-laminar sublayer model
J_o	J for ordinary fluids
ℓ	Mixing length
ℓ^*	Nondimensional mixing length, $\ell^* = u_\tau \ell/\nu$
$\hat{\ell}$	Characteristic additive length
m	Characteristic additive mass
q	Wake modification function
R	Pipe Reynolds number, $R = VD/\nu$
r	Radius of pipe, $r = D/2$
r^*	Nondimensional radius, $r = u_\tau r/\nu$
t	Characteristic additive time
U	Velocity at pipe center
u	Velocity at point in pipe
u_τ	Shear velocity, $u_\tau = \sqrt{\tau_w/\rho}$
u^*	Nondimensional velocity, $u^* = u/u_\tau$

u^*_1	u^* for laminar sublayer, buffer layer and logarithmic layer extendfed to pipe center
u^*_2	Correction to u^*,$u^*_2 = u^* - u^*_1$
V	Average velocity across pipe
w	Wake function
y	Radial distance from pipe wall
y^*	Nondimensional y, $y^* = u_\tau y/\nu$
y_o^*	y^* for thickness of extended viscous sublayer
y_L^*	y^* for thickness of laminar sublayer
$\widetilde{y_L}^*$	y_L^* for elastic-layer model
y_m^*	y^* for thickness of elastic layer
α,β	Constants
ΔB	Drag reduction characterization, $\Delta B = B_1 - B_{1,0}$
κ	von Kármán constant, $\kappa = 1/A$
λ	van Driest factor
$\widetilde{\lambda}$	Darcy-Weisbach friction factor
λ^*	Nondimensional van Driest factor,$\lambda^* = u_\tau \lambda/\nu$
ρ	Density of fluid
ν	Kinematic viscosity of fluid
τ	Shear stress in fluid
τ_t	Turbulent shear stress
τ_w	Wall shear stress
τ^*	Nondimensional shear stress, $\tau^* = \tau/\tau_w$
f	Function of

5

ABSTRACT

The method of two loci for scaling-up the drag reduction by additives from measurements in not-too-small diameter pipes to large diameter pipes is extended to small diameter pipes. This is accomplished by including the effects of the viscous sublayer and buffer layer in formulating a prediction chart. A mixing-length model proved more accurate than three other models of the viscous sublayer and buffer layer in a comparison of predictions with measured data. The prediction chart may also be used to obtain a similarity-law drag-reduction characterization.

INTRODUCTION

The prediction of drag reduction by additives* in large diameter pipes from measurements in small diameter pipes using the method of two loci[1] has been shown by Sellin and Ollis[2] to be accurate when the diameters of the test pipes are sufficiently large. From an engineering viewpoint, it may be more economical to use small pipes to measure the actual drag reduction characteristics of commercially available additives which may vary in molecular sizes due to the manufacturing process. It is the intention of this paper to extend the method of two loci to small pipes by including the effects of the viscous sublayer and the buffer layer which were not included in the original method developed for large pipes[1].

The problem of scaling-up the results from smaller pipes to larger pipes arises from a two-parameter variation of the friction factor with not only the usual Reynolds-number dependence but also a nondimensional diameter for the same concentration and species of additive[1]. Fortunately, the classical velocity similarity laws[3,4] provide a characterization of drag reduction which is

* Most of the material in this paper was presented to the Third International Conference on Drag Reduction, July 2-5, 1984 at the University of Bristol, England.

independent of pipe diameter. The original method of two loci[1] considered the logarithmic similarity law to be valid up to the wall, thus ignoring the effects of the viscous sublayer and buffer layer. The method was hence applicable to large pipes only. By including the effects of the viscous sublayer and buffer layer, the method of two loci can be extended to small pipes. Four existing models of the similarity laws for the viscous (laminar) sublayer and the buffer layer are to be considered, namely,

1. A variable thick laminar sublayer and an associated buffer layer[3];
2. A constant laminar sublayer and an elastic layer in lieu of the buffer layer[5];
3. A mixing-length formulation[6,7]; and
4. An extended viscous sublayer[8].

A brief review of the velocity similarity laws is presented. The four models are used to obtain four friction-factor formulations. The results are presented graphically fo~ the extended method of two loci. Predictions from the four models are compared with experimental data. An appendix shows how to determine a similarity-law drag characterization from small-diameter pipe flows.

VELOCITY SIMILARITY LAWS

In general, the inner similarity laws for drag-reducing additives (3) may be stated nondimensionally as

$$u^* = f\left[y^*, \frac{u_\tau \hat{\ell}}{\nu}, C, \hat{A}\right] \tag{1}$$

where $u^* = u/u_\tau$; u = mean turbulent velocity parallel to the pipe wall; $u_\tau = \sqrt{\tau_w/\rho}$; τ_w = wall shearing stress; ρ = density of fluid; $y^* = u_\tau y/\nu$; y = normal distance from the wall; ν = kinematic viscosity of fluid; $\hat{\ell}$ = characteristic length representing the additive; C = concentration of additive; $\hat{A}$ = species or kind of additive. The characteristic length $\hat{\ell}$ in this paper serves mostly as a dummy variable.

A characteristic time t or mass m may be substituted for the characteristic length $\hat{\ell}$ where $\hat{\ell} = \sqrt{t\nu} = (m\rho)^{1/3}$.

The outer similarity law which does not directly depend on the presence of additives may be stated for fully developed pipe flow as

$$\frac{U-u}{u_\tau} = f\left[\frac{y}{r}\right] \tag{2}$$

where U = velocity at the center of the pipe and r = radius of the pipe.

The overlapping of the inner and outer laws results in logarithmic laws

$$u^* = A \, \ln y^* + B_1 \tag{3}$$

or

$$\frac{U-u}{u_\tau} = -A \ln \frac{y}{r} + B_2 \tag{4}$$

where

$$B_1 = f\left[\frac{u_\tau \hat{l}}{\nu}, C, \hat{A}\right] \tag{5}$$

may be termed the drag-reduction characterization. Another drag-reduction characterization is

$$\Delta B = B_1 - B_{1,0} = f\left[\frac{u_\tau \hat{l}}{\nu}, C, \hat{A}\right] \tag{6}$$

where $B_{1,0}$ = value of B_1 in the absence of the additive. A and B_2 are constants for pipe flow.

If the logarithmic velocity law, Equation (3) is considered to extend to the pipe center, a correction has to be applied. The nondimensional velocity u^* across the pipe is to be represented by two components

$$u^* = u_1^* + u_2^* \tag{7}$$

where u_1^* is the contribution of the laminar (viscous) sublayer, the buffer layer and the logarithmic layer extended to the pipe center.

u_2^* is the correction represented by

$$u_2^* = B_2 \frac{w}{2} + A q \tag{8}$$

where $\frac{w}{2}$ is the Coles wake function and q is the wake modification function[9].

Polynomial fits to w/2 and q are given by

$$\frac{w}{2} = 3\left(\frac{y^*}{r^*}\right)^2 - 2\left(\frac{y^*}{r^*}\right)^3 \qquad (9)$$

and

$$q = \left(\frac{y^*}{r^*}\right)^2 - \left(\frac{y^*}{r^*}\right)^3 \qquad (10)$$

where $r^* = u_\tau r/\nu$

PIPE FLOW

For the fully-developed flow of drag-reduction solutions through pipes the Fanning friction factor f may be stated functionally as

$$f = f\left[R,\ D/\hat{\ell},\ C,\ \hat{A}\right] \qquad (11)$$

where f = Fanning friction factor = $2\tau_w/\rho V^2$; V = average velocity across the pipe; R = pipe Reynolds number = VD/ν; D = diameter of the pipe = 2r.

For the same concentration C and species $\hat{A}$ of additive, the friction factor varies not only with Reynolds number R but also with nondimensional diameter $D/\hat{\ell}$; hence the scale-up problem. Another commonly used friction factor is the Darcy-Weisbach friction factor $\tilde{\lambda}$ where*

$$\tilde{\lambda} = 4f \qquad (12)$$

The average velocity V across a circular pipe may be determined from the similarity-law velocity profile by means of

$$\frac{V}{u_\tau} = \frac{2}{r^*}\left(\int_0^{r^*} u^*\, dy^* - \frac{1}{r^*}\int_0^{r^*} u^*\, y^*\, dy^*\right) \qquad (13)$$

which is derived in Reference 3.

Also by definition

$$\frac{V}{u_\tau} = \sqrt{\frac{2}{f}} \qquad (14)$$

---

*Note that hydraulic engineers seem to prefer the Darcy-Weisbach friction factor using either the symbol f or λ. Chemical engineers seem to prefer the Fanning friction factor using the symbol f as used here.

and

$$r^* = \frac{\sqrt{2}}{4}\left(\sqrt{f}\, R\right) \tag{15}$$

which bridge similarity-law variables and pipe variables.

EXTENDED METHOD OF TWO LOCI

If the logarithmic velocity law, Equation (3), is assumed to hold up to the wall, that is, without any effect from the viscous sublayer and the buffer layer, then by means of Equations (7), (8), (9), and (10) there results

$$\frac{1}{\sqrt{f}} = \frac{A}{\sqrt{2}} \ln \sqrt{f}\, R - \frac{1}{\sqrt{2}}\left(A \ln \sqrt{8} + \frac{43}{30} A - B_{1,0} - \frac{3}{10} B_2\right) + \frac{\Delta B}{\sqrt{2}} \tag{16}$$

For ordinary fluids ($\Delta B = 0$), this equation has the same form as the well-known Prandtl-Karman formula for pipe flow

$$\frac{1}{\sqrt{f}} = 4.0 \log_{10} \sqrt{f}\, R - 0.4 \tag{17}$$

Now for the same concentration C and species $\hat{A}$ of additive the similarity-law characterization ΔB is

$$\Delta B = f\left[\frac{u_\tau \hat{\ell}}{\nu}\right] \tag{18}$$

Hence the values of both ΔB and $\frac{u_\tau \hat{\ell}}{\nu}$ have to be satisified for pipes of different diameters.

It is obvious that, for a plot of $1/\sqrt{f}$ against $\sqrt{f}\, R$, lines of constant ΔB are parallel to each other in accordance with Equation (16). This is the first locus which only applies to sufficiently large pipes where the effects of the viscous sublayer and the buffer layer are negligible.

The second locus has to satisfy the same value of $u_\tau \hat{\ell}/\nu$, which by definition is

$$\frac{u_\tau \hat{l}}{\nu} = \frac{1}{\sqrt{2}}\left(\sqrt{f}\,R\right)\left(\frac{\hat{l}}{2r}\right) \tag{19}$$

For the same concentration and species, $\hat{\ell}$ is constant. Thus in going from pipe diameter D_1 to pipe diameter D_2, for the same value of $u_\tau \hat{\ell}/\nu$,

$$\left(\sqrt{f}\,R\right)_2 = \left(\sqrt{f}\,R\right)_1 \left(\frac{D_2}{D_1}\right) \tag{20}$$

This represents the second locus which does not exclude the effects of the viscous sublayer and the buffer layer.

For smaller pipes where the effects of the viscous (laminar) sublayer and the buffer layer are not negligible, the lines of constant ΔB on a $1/\sqrt{f}$ - $\sqrt{f}R$ plot are no longer straight and parallel. Hence the curved lines of constant ΔB have to be plotted at sufficiently close intervals so that the locus of constant ΔB is drawn from a measured point by interpolating between two nearby lines of constant ΔB. This is shown in Figure 1.

Four analytical models of the viscous (laminar) sublayer and the buffer layer are now to be examined in order to determine the curved lines of constant ΔB.

THICK LAMINAR SUBLAYER

The first analytical model proposed for the buffer layer seems to be that of reference 3 which was based on an eddy viscosity model. The result is a laminar sublayer which thickens with increasing values of ΔB.

As usual the laminar sublayer of thickness y_L^* is given by

$$u_1^* = y^*, \quad 0 < y^* < y_L^* \tag{21}$$

Outside the laminar sublayer a logarithmic relation holds for both the buffer layer and the logarithmic layer which is

$$u_1^* = A \ln(y^* - J) + B_1, \quad y^* > y_L^* \tag{22}$$

This relation joins the laminar sublayer in both value and derivative. The result is

$$J = B_1 - A + A \ln A \tag{23}$$

$$y_L^* = B_1 + A \ln A \tag{24}$$

and for ordinary fluids

$$J_0 = B_{1,0} - A + A \ln A \tag{25}$$

Determining the average velocity from Equation (13) and converting to $\sqrt{f}$ and $\sqrt{f}R$ coordinates yields

$$\frac{1}{\sqrt{f}} = \frac{A}{\sqrt{2}} \ln \sqrt{f}R - \frac{1}{\sqrt{2}}\left(A \ln \sqrt{8} + \frac{43}{30}A - B_{1,0} - \frac{3}{10}B_2\right) + \frac{\Delta B}{\sqrt{2}} - \frac{\alpha}{\sqrt{f}R} + \frac{\beta}{(\sqrt{f}R)^2} \tag{26}$$

where

and

$$\alpha = 2\left[2A(J_0 + \Delta B)\ln(\sqrt{f}R/\sqrt{8}) + 2(J_0 + \Delta B)(B_{1,0} + \Delta B) - (J_0 + A + \Delta B)^2\right]$$

$$\beta = 4\sqrt{2}\left[A(J_0 + \Delta B)\ln(\sqrt{f}R/\sqrt{8}) + (J_0 + \Delta B)^2(A + B_{1,0} + \Delta B) + \frac{A^3}{2} + A^2(J_0 + \Delta B) - \frac{2}{3}(J_0 + A + \Delta B)^3\right]$$

It is to be noted that this equation is the same as that of Equation (16) except for the added terms due to the laminar sublayer and the buffer layer which decrease as $\sqrt{f}R$ increases for larger diameter pipes.

ELASTIC LAYER

On the basis of a line of maximum drag-reduction in pipe flow, Virk et al[5] proposed a logarithmic relation for the buffer layer, which was renamed the elastic layer, of the form

$$u^* = \tilde{A} \ln y^* - \tilde{B} \tag{27}$$

where $\tilde{A}$ and $\tilde{B}$ are constants. This relation begins at the intersection of the logarithmic line and laminar line for the ordinary fluids, $\tilde{y}_L^*$. As stated, no buffer layer is allowed for ordinary fluids so that $\tilde{y}_L^*$ is a constant.

For drag-reducing fluids the elastic line ends at y^*_m which is the intersection of the elastic line and the logarithmic line or

$$y^*_m = \exp\left[\frac{B_{1,0} + \tilde{B} + \Delta B}{\tilde{A} - A}\right] \tag{28}$$

Performing the required integrations of Equation (13) results in

$$\frac{1}{\sqrt{f}} = \frac{A}{\sqrt{2}} \ln \sqrt{f}R - \frac{1}{\sqrt{2}}\left(A \ln \sqrt{8} + \frac{43}{30}A - B_{1,0} - \frac{3}{10}B_2\right) + \frac{\Delta B}{\sqrt{2}} - \frac{\alpha}{\sqrt{f}R} + \frac{\beta}{(\sqrt{f}R)^2} \tag{29}$$

where

$$\alpha = 2\left[2(\tilde{A} - A)y^*_m + \tilde{y}_L^{*2} - 2A\,y^*_L\right]$$

and

$$\beta = 4\sqrt{2}\left[\frac{(\tilde{A}-A)}{2} y_m^{*2} + \frac{\tilde{y}_L^{*3}}{3} - \frac{A}{2}\tilde{y}_L^{*2}\right]$$

Recently this elastic-layer formulation was used in an iterative calculation method by Matthys and Sabersky[10] in scaling-up pipe data.

MIXING LENGTH

Poreh and Dimant[6,7] extended the Prandtl-van Driest mixing-length formulation to drag-reducing solutions as follows. Both the viscous sublayer and buffer layer are included.

According to mixing-length theory the turbulent shear stress τ_t is related to the velocity gradient as

$$\frac{\tau_t}{\rho} = \ell^2 \left(\frac{du}{dy}\right)^2 \tag{30}$$

where ℓ is the mixing length.

Including the laminar shear stress results in nondimensional terms as

$$\tau^* = \ell^{*2}\left(\frac{du^*}{dy^*}\right)^2 + \frac{du^*}{dy^*} \tag{31}$$

where $\tau^* = \tau/\tau_w$, $\ell^* = u_\tau \ell/\upsilon$ and τ = shear stress in fluid.

Solving as a quadratic quation yields a velocity profile

$$u^* = \int_0^{y^*} \frac{2\tau^*}{1+\sqrt{1+(2\ell^*)^2\tau^*}}\, dy^* \tag{32}$$

The Prandtl-van Driest mixing-length formulation is nondimensionally

$$\ell^* = \kappa y^* \left(1 - \frac{1}{e^{y^*/\lambda^*}}\right) \tag{33}$$

where κ = von Kármán constant = 1/A; $\lambda^* = u_\tau \lambda/\upsilon$ and λ = van Driest factor.

For pipe flow the shear stress is given as

$$\tau^* = 1 - \frac{y^*}{r^*} \tag{34}$$

The van Driest factor λ^* may be correlated with the drag-reduction characterization B_1 or ΔB as follows.

At high values of r^* where $\tau^* = 1$ and where the mixing-length velocity profile, Equation (32), merges into the logarithmic velocity profile

$$B_1 = \int_0^{\tilde{y}^*} \frac{2}{1+\sqrt{1+\left[2\kappa y^*\left(1-e^{-y^*/\lambda^*}\right)\right]^2}}\, dy^* - A \ln \tilde{y}^* \tag{35}$$

where $\tilde{y}^*$ is a sufficiently large value of y^*. B_1 is thus a function of λ^*.

If Equation (32) is considered to extend to the pipe center, u^* becomes u_1^* and the outer correction u_2^*, as assumed by Poreh and Dimant, is

$$u_2^* = B_2 \frac{w}{2}\left[1-\exp\left(-2r^*/\lambda^*\right)\right] \tag{36}$$

The evaluation of the average velocity bv Equation (13) has to proceed numerically in order to develop a $1/\sqrt{f}$ vs. $\sqrt{f}R$ relationship. Tiederman and Reischman[11] show that the Prandtl-van Driest mixing-length formulation indirectly fits the measured velocity profiles. The eddy viscosity relationship actually used by them may be shown to be based on the Prandtl-van Driest mixing length.

EXTENDED VISCOUS SUBLAYER

An extended viscous sublayer proposed by Wasan for ordinary fluids was applied to drag-reducing fluids by Kwack and Hartnett[8]. The effect of an eddy viscosity was added to the laminar flow to give a velocity profile for both the viscous sublayer and the buffer layer such that

$$u^* = y^* + c_1 y^{*4} + c_2 y^{*5} \tag{37}$$

where c_1 and c_2 are constants to be determined. The fourth power of y^* is chosen to provide a third-power variation of eddy viscosity with y at the wall. The junction of Equation (37) with the logarithmic law, Equation (3), is at y_0^*.

The values of c_1, c_2 and y_0^* vary wth B_1 or ΔB and are determined by continuity at the junction y_0^* so that

$$c_1 = -\frac{1}{y_0^{*3}} + \frac{5A}{4y_0^{*4}} \tag{38}$$

$$c_2 = \frac{3}{5y_0^{*4}} - \frac{4A}{5y_0^{*5}} \tag{39}$$

and $$B_1 = \frac{3y_o^{\alpha}}{5} - A \ln y_o^{\alpha} + \frac{9A}{20} \tag{40}$$

Using Eq. (13) and converting to $\sqrt{f}$ and $\sqrt{f}R$ coordinates results in

$$\frac{1}{\sqrt{f}} = \frac{A}{\sqrt{2}} \ln \sqrt{f} R - \frac{1}{\sqrt{2}}\left(A \ln \sqrt{8} + \frac{43}{30}A - B_{1,0} - \frac{3}{10}B_2\right) + \frac{\Delta B}{\sqrt{2}} - \frac{\alpha}{\sqrt{f}R} + \frac{\beta}{(\sqrt{f}R)^2} \tag{41}$$

where

$$\alpha = 4\left[-A y_o^{\alpha} + \frac{y_o^{\alpha^2}}{2} + \frac{4C_1}{5} y_o^{\alpha^5} + \frac{5C_2}{6} y_o^{\alpha^6}\right]$$

and

$$\beta = 4\sqrt{2}\left[-\frac{A\, y_o^{\alpha^2}}{2} + \frac{y_o^{\alpha^3}}{3} + \frac{2C_1}{3} y_o^{\alpha^6} + \frac{5C_2}{7} y_o^{\alpha^7}\right]$$

NUMERICAL AND GRAPHICAL RESULTS

Charts for Method of Two Loci

The charts for the extended method of two loci are shown in Figures 2,3,4, and 5 for the thick laminar-sublayer model, the elastic-layer model, the mixing-length model, and the extended viscous-sublayer model respectively.

For the case of ordinary fluids, $\Delta B = 0$, the usual Prandtl-Karman formula, Equation (17), is plotted. Values of $A = 2.5$, $B_{1,0} = 5.5$, $\tilde{A} = 11.7$, $\tilde{B} = 17.0$ are used in the calculations for the thick laminar-sublayer model, the elastic-layer model and the extended viscous sublayer model. A value of $\tilde{y}_L^* = 11.6$ is used for the elastic-layer model.

The chart for the mixing-length model is developed from a graph of computed results presented by Dimant and Poreh (7).

Comparison of Predictions

The experimental data of Sellin and Ollis (2) for the drag-reduction in a 5 mm diameter pipe and in a 50 mm diameter pipe are used to compare predictions from the three methods in scaling-up the data from the 5mm to the 50 mm pipe. The measured data are for a 10 wpm concentration of a commercial polyacrylamide, Alcomer-110L. Solid symbols represent experimental data while open symbols represent predictions.

As shown in Figures 2, 3, 4 and 5, the mixing-length model gives excellent predictions for the few data presented. The thick laminar-sublayer, the elastic-layer and extended viscous-sublayer models show a poor comparison between predicted and measured data. This seems to indicate that the mixing-length model gives the best representation of the viscous sublayer and buffer layer.

CONCLUDING REMARKS

The inclusion of the effects of the viscous (laminar) sublayer and the buffer layer definitely seems to improve the accuracy of the original method of two loci especially for small-diameter pipes. This may be seen by noting the curved lines of constant ΔB in the $1/\sqrt{f}$ vs. $\sqrt{f}R$ plot which deviate from the straight lines specified in the original method of two loci. At higher values of $\sqrt{f}R$, which apply to large diameter pipes. the lines of constant ΔB start to become straight and parallel in accordance with the original method of two loci. This explains the success of Sellin and Ollis (2) in making predictions from 25 to 50 mm diameter pipes and the lack of success in making predictions from smaller than 25 mm diameter pipes.

The van Driest mixing-length model gives predictions in scaling-up the data from 5 mm diameter pipe to a 50 mm pipe which agree well with the available experimental data. Hence the van Driest model as given in Figure 4 is recommended for the extended method of two loci.

REFERENCES

1. Granville, P.S., "Scaling-up of Pipe-Flow Frictional Data for Drag-Reducing Polymer Solutions," 2nd International Conference on Drag Reduction, Cambridge, England, Aug. 31, 1977.

2. Sellin, R.H.J. and M. Ollis, "Effect of Pipe Diameter on Polymer Drag Reduction," Industrial and Engineering Chemistry, Product Research and Development, Vol. 22, No. 3, pp. 445-452 (Sep 1983).

3. Granville, P.S., "Frictional Resistance and Velocity Similarity Laws of Drag-Reducing Polymer Solutions," Journal of Ship Research, Vol. 12, No. 3, pp. 201-222 (Sep 1968).

4. Huang, T.T., "Similarity Laws for Turbulent Flow of Dilute Solutions of Drag-Reducing Polymers," Physics of Fluids, Vol. 1, No. 2, pp. 298-309 (Feb 1974).

5. Virk, P.S., H.S Mickley and K.A. Smith, "The Ultimate Asymptote and Mean Flow Structure in Toms' Phenomenon," Journal of Applied Mechanics (ASME), Vol. 37, Series E, No. 2, pp. 488-493 (June 1970).

6. Poreh, M. and Y. Dimant, "Velocity Distribution and Friction Factors in Flows with Drag Reduction," 9th Symposium on Naval Hydrodynamics, Paris, August 1972, ACR-203, U.S. Government Printing Office, Washington, D.C.

7. Dimant, Y. and M. Poreh, "Momentum and Heat Transfer in Flows With Drag Reduction," Publication 203, Faculty of Civil Engineering, Israel Institute of Technology (March 1974).

8. Kwack, E.Y. and J.P. Hartnett, "Estimated Eddy Diffusivities of Momentum and Heat of Viscoelastic Fluids," International Journal of Heat and Mass Transfer, Vol. 27, No. 9, pp. 1525-1531 (Sep 1984).

9. Granville, P.S., "A Modified Law of the Wake for Turbulent Shear Flows," Journal of Fluids Engineering (ASME), Vol. 98, No. 3, pp. 578-580 (Sep 1976).

10. Matthys, E.F. and R.H. Sabersky, "A Method of Predicting the Diameter Effect for Heat Transfer and Friction of Drag-Reducing Fluids," International Journal of Heat & Mass Transfer, Vol. 25, No. 9, pp. 1343-1351 (Sep 1982).

11. Tiederman, W.G. and M.M. Reischman, "Calculation of Velocity Profiles in Drag-Reducing Flows," Journal of Fluids Engineering (ASME), Vol. 98, Series I, No. 3, pp. 563-566, (Sep 1976).

APPENDIX

DETERMINATION OF SIMILARITY-LAW DRAG-REDUCTION CHARACTERIZATION

The ΔB-characterization may be also determined from the chart, $1/\sqrt{f}$ vs. $\sqrt{f}R$ and ΔB, as a function of $u_\tau \hat{\ell}/\nu$ for the particular concentration and type of additive involved.

The test point $(1/\sqrt{f}, \sqrt{f}R)$ for a particular diameter pipe D gives the ΔB value from an interpolation between the lines of constant ΔB.

From definition, the value of $\frac{u_\tau \hat{\ell}}{\nu}$ is given here as

$$\frac{u_\tau \hat{\ell}}{\nu} = \frac{\sqrt{2}}{2} \sqrt{f}R \cdot \frac{\hat{\ell}}{D} \tag{A1}$$

In many applications, the characteristic length $\hat{\ell}$ serves as a dummy quantity. The ΔB characterization may then be used to determine the viscous drag of bodies by a boundary-layer calculation.

FIGURE 1 - Extended Method of Two Loci

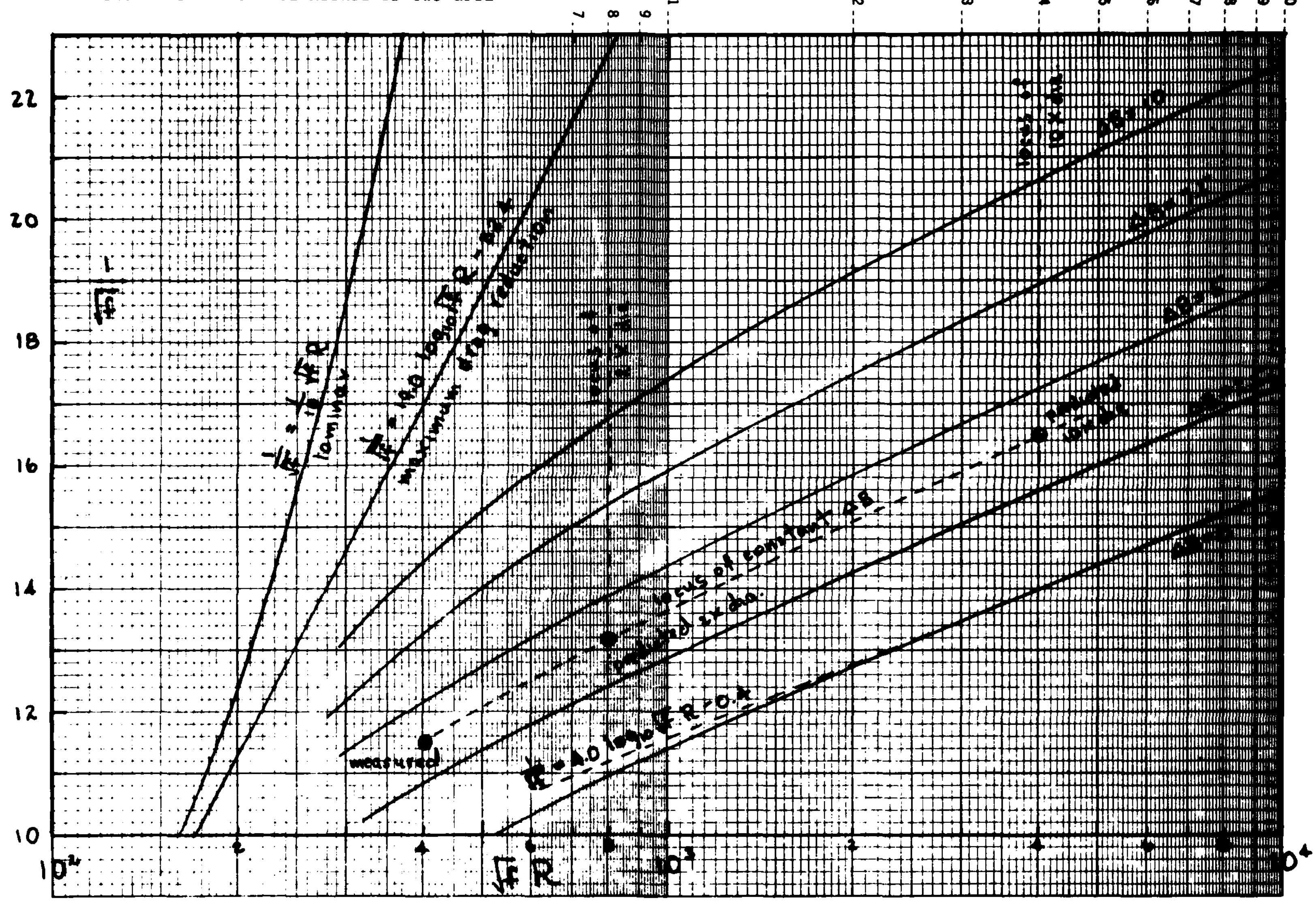

K•E SEMI-LOGARITHMIC • 2 CYCLES × 70 DIVISIONS KEUFFEL & ESSER CO. MADE IN U.S.A. 46 4970

FIGURE 2 - Method of Two Loci for Thick Laminar-Sublayer Model

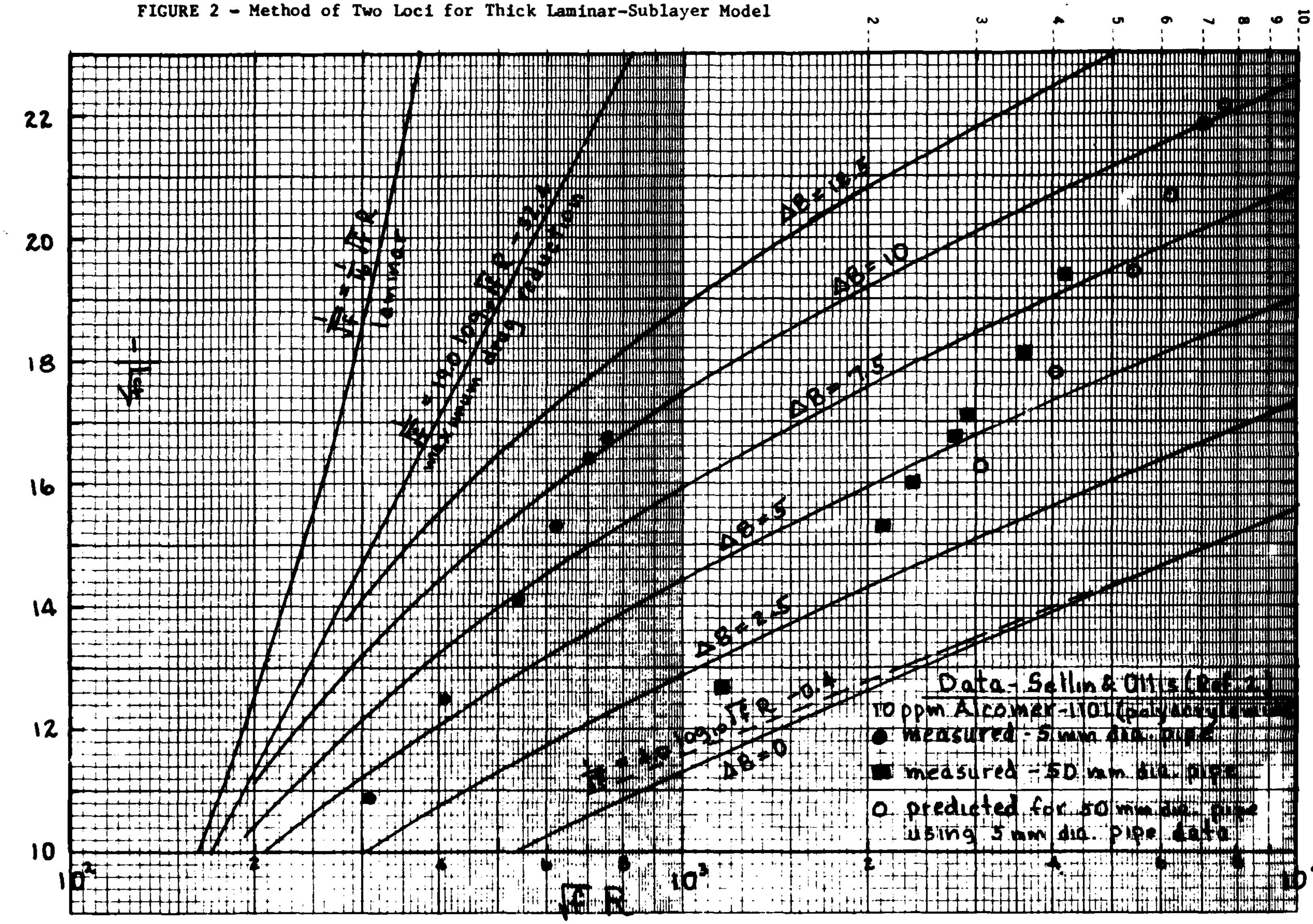

FIGURE 3 - Method of Two Loci for Elastic-Layer Model

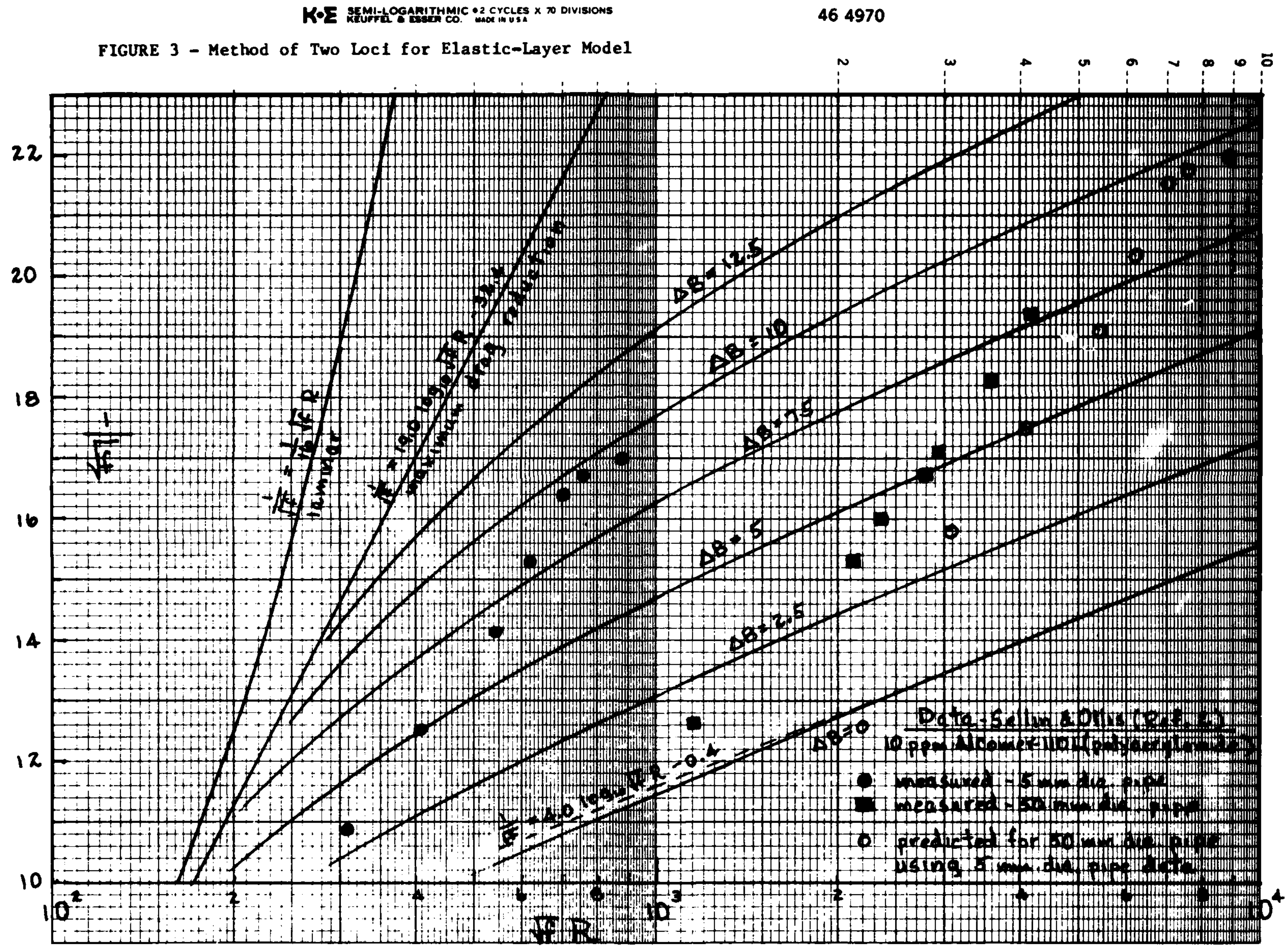

K•E SEMI-LOGARITHMIC CYCLES X 70 DIVISIONS KEUFFEL & ESSER CO. MADE IN U.S.A. 46 4970

FIGURE 4 - Method of Two Loci for Mixing-Length Model

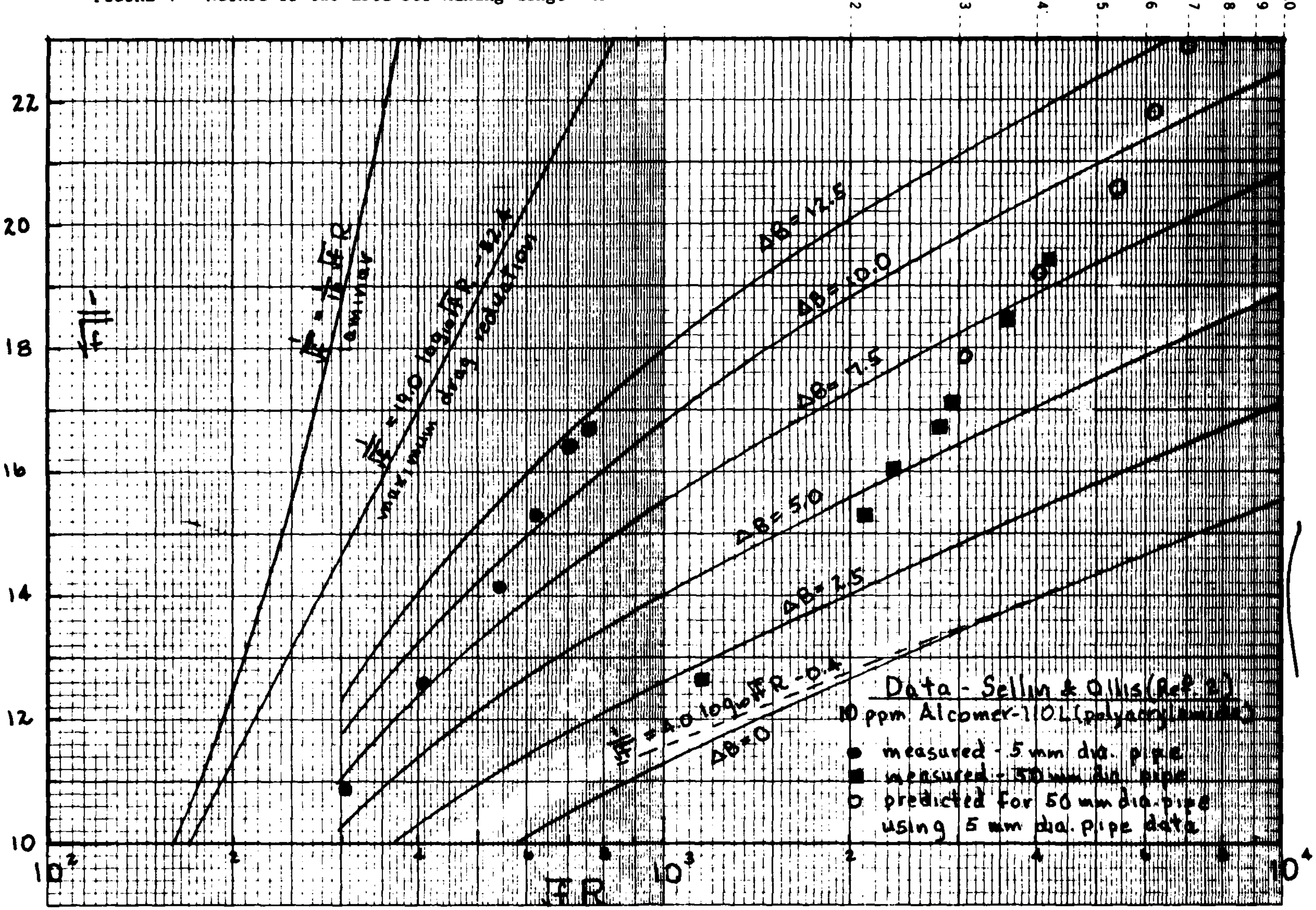

FIGURE 5 - Method of Two Loci for Extended Viscous-Sublayer Model

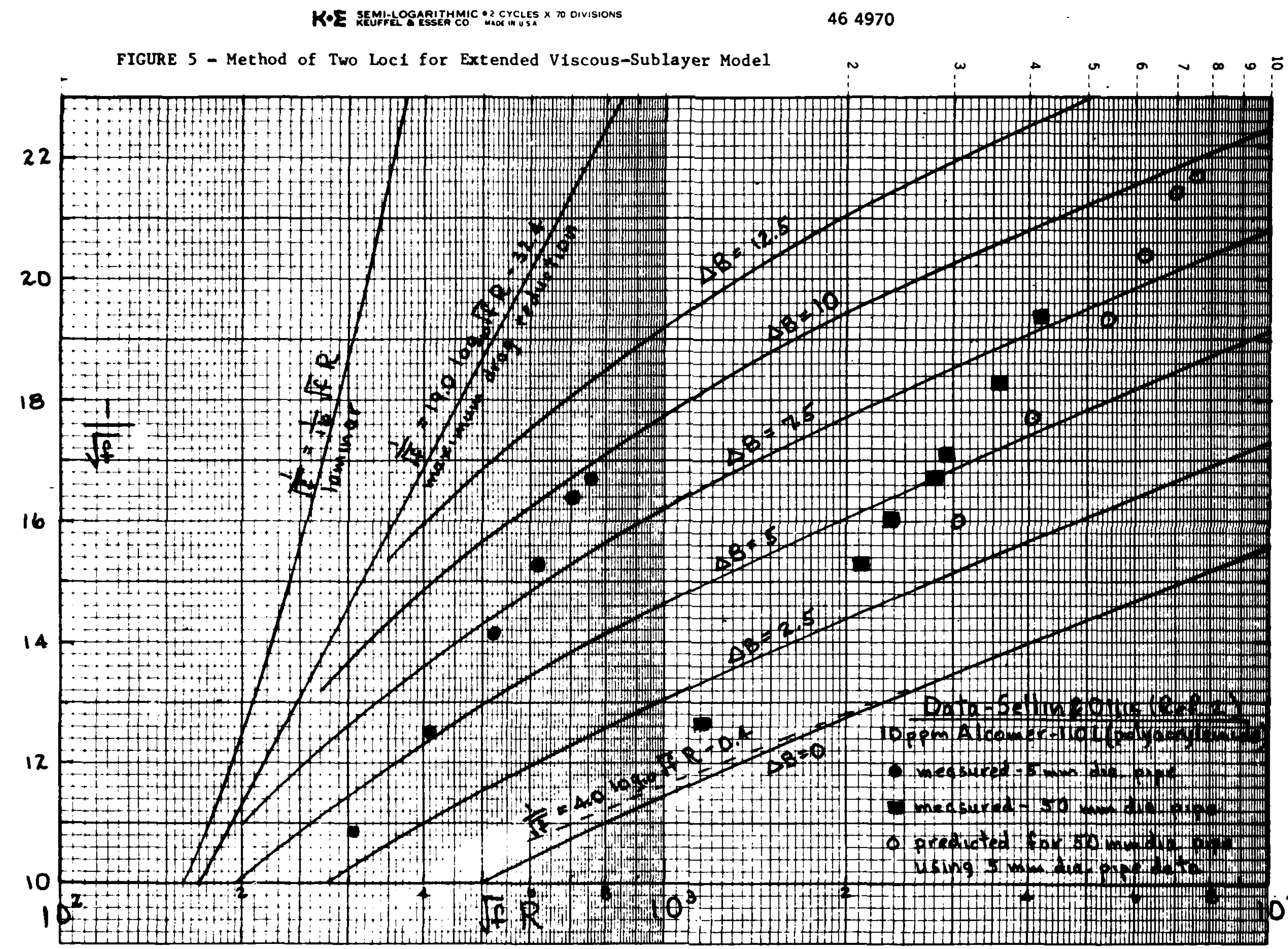

DTNSRDC ISSUES THREE TYPES OF REPORTS

1. DTNSRDC REPORTS, A FORMAL SERIES, CONTAIN INFORMATION OF PERMANENT TECHNICAL VALUE. THEY CARRY A CONSECUTIVE NUMERICAL IDENTIFICATION REGARDLESS OF THEIR CLASSIFICATION OR THE ORIGINATING DEPARTMENT.

2. DEPARTMENTAL REPORTS, A SEMIFORMAL SERIES, CONTAIN INFORMATION OF A PRELIMINARY, TEMPORARY, OR PROPRIETARY NATURE OR OF LIMITED INTEREST OR SIGNIFICANCE. THEY CARRY A DEPARTMENTAL ALPHANUMERICAL IDENTIFICATION.

3. TECHNICAL MEMORANDA, AN INFORMAL SERIES, CONTAIN TECHNICAL DOCUMENTATION OF LIMITED USE AND INTEREST. THEY ARE PRIMARILY WORKING PAPERS INTENDED FOR INTERNAL USE. THEY CARRY AN IDENTIFYING NUMBER WHICH INDICATES THEIR TYPE AND THE NUMERICAL CODE OF THE ORIGINATING DEPARTMENT. ANY DISTRIBUTION OUTSIDE DTNSRDC MUST BE APPROVED BY THE HEAD OF THE ORIGINATING DEPARTMENT ON A CASE-BY-CASE BASIS.

END

FILMED

6-85

DTIC